Int J Clin Exp Med 2018;11(9):9851-9857
www.ijcem.com /ISSN:1940-5901/IJCEM0069856

Original Article

Value of dynamic contrast-enhanced magnetic resonance imaging in predicting lymph node metastasis in cervical cancer

Junwen Huang, Jiacheng Song, Yan Li, Zhanlong Ma, Haibin Shi

Department of Radiology, First Affiliated Hospital of Nanjing Medical University, Nanjing, China

Received July 23, 2017; Accepted April 14, 2018; Epub September 15, 2018; Published September 30, 2018

Abstract: Background: To compare the changes of dynamic contrast-enhanced magnetic resonance imaging (DCE-MRI) quantitative parameter in cervical cancer patients with and without lymph node metastasis. Methods: Fifty-eight patients with cervical cancer underwent DCE-MRI before operation, twenty-eight of those cases presented with lymph node metastasis, and thirty cases presented without lymph node metastasis. All cases had diagnoses confirmed by pathology. DCE-MRI parameters were calculated for the tumour. Additionally, apparent diffusion coefficient (ADC) value was analyzed. Then, all patients were followed for two year. Results: The K^{trans} and V_e value were significantly higher in the tumour with lymph node metastasis than in the tumour without lymph node metastasis (1.446±0.129 vs. 1.047±0.114 min^{-1}, p = 0.023; and 0.730±0.038 vs. 0.571±0.045%, p = 0.010; respectively). In addition, the ADC value also showed a significant difference between the two groups (0.694±0.020 vs. 0.776±0.035×10^{-3} mm^2/s, p = 0.044). During the two-year follow-up period, there were two cases of distant metastases in patients with lymph node metastasis. Conclusion: K^{trans} and V_e of DCE-MRI are useful for predicting the probability of lymph node metastasis in cervical cancer patients. In addition, the ADC value is an effective and necessary supplementation for predicting lymph node metastasis.

Keywords: DCE-MRI, quantitative parameters, cervical cancer, lymph node metastasis, ADC

Introduction

Cervical cancer is the most common gynecological malignancy, and the second most frequent cause of cancer death in Chinese women [1]. Generally, patients with risk factors, such as positive lymph nodes, parametrial invasion or a positive vaginal margin are regarded as being at a "high risk" of recurrence [2]. Although the status of lymph nodes is not included in the International Federation Gynecology and Obstetrics (FIGO) stages, it remains an important factor in determining the appropriate treatment plan, and is consistently associated with poor survival [3]. Unfortunately, a significant portion of patients present with clinically and radiographically silent lymph node metastasis at time of diagnosis. The study of risk factors related to lymph nodes can help to identify patients who are more likely to have lymph node involvement, to assess the prognosis and to guide individualized radiotherapy [4, 5].

Dynamic contrast-enhanced magnetic resonance imaging (DCE-MRI) is a non-invasive imaging technique that can characterize tissue vasculature and is sensitive to differences in blood volume and vascular permeability that can be related to tumour angiogenesis [6]. In cervical cancers, several studies reported that DCE-MRI could potentially evaluate the metastatic potential of enlarged lymph nodes on MR imaging [7]. Until now, few studies have reported the value of DCE-MRI quantitative parameter of tumour to predict lymph node metastasis.

To that end, the current study seeks to evaluate the potential of DCE-MRI quantitative parameter to identify lymph node metastasis in cervical cancer patients.

Patients and methods

Study population

This retrospective study was approved by our institutional review board and the requirement

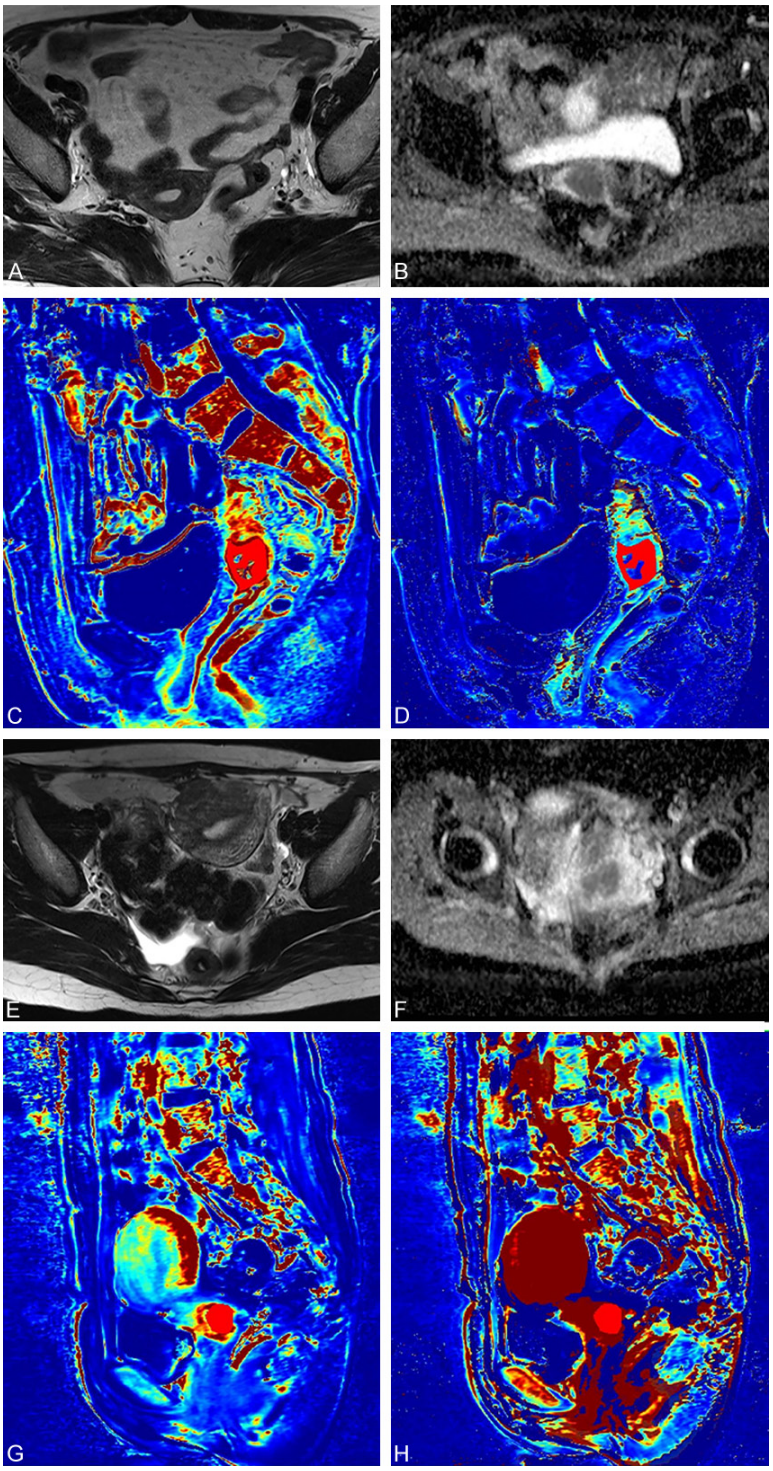

Figure 1. (A-D) A 25-year-old woman in cervical cancer (FIGO staging Ib) with lymph node metastasis. Axial T1W image shows no enlarged lymph node in the left pelvic cavity (A). Axial ADC map, the tumor is clearly defined with a low signal (B). Estimated DCE parameters are as follows: K^{trans} = 1.280 min^{-1} (C), V_e = 0.997% (D). (E-H) A 65-year-old woman in cervical cancer (FIGO staging Ib) without lymph node metastasis. Axial T1W image shows an enlarged lymph node (E). Axial ADC map, the tumor is clearly defined with a low signal (F). Estimated DCE parameters are as follows: K^{trans} = 0.298 min^{-1} (G), V_e = 0.352% (H).

for informed consent was waived. We retrospectively studied 58 patients with cervical cancer who had undergone operation at the Jiangsu Province People's Hospital between January 2013 and December 2016. All patients were staged according to the 2009 FIGO staging system. All tissue specimens and slides were examined by experienced pathologists. The lymph node metastasis that were pathologically confirmed either underwent operation resection. All patients had complete MR imaging, including DCE-MRI before operation. Clinical and pathological data, including age, FIGO stage, histological type, tumour volume and carcinoembryonic antigen (CEA) were examined. Patients with the following criteria were excluded: (a) patients receiving any neoadjuvant treatment; (b) DCE-MRI not included in the MRI of the pelvic; (c) patients who were lost to follow-up; or (d) images showing unacceptable distortion due to artefacts from metallic clips around the tumour.

MR imaging technique

All imaging examinations were performed with 3.0T MR scanners (MAGNETOM Trio-Tim; Siemens, Erlangen, Germany) using a 16-element pelvic phased-array coil. As per the standard pelvic MRI protocol at our institution, the images obtained included transverse T1-weighted turbo spin-echo (TSE) images (TR/TE, 993/26 msec; section thickness, 3.5 mm; field of view [FOV], 250) and transverse (TR/TE, 4430/129 msec; section thickness, 3.5 mm;

FOV, 250), coronal (TR/TE, 4000/77 msec; section thickness, 4.0 mm; FOV, 300), and sagittal (TR/TE, 4000/129 msec; section thickness, 3.0 mm; FOV, 250) T2-weighted TSE images of the uterus. Then single-shot echo-planar imaging (TR/TE, 6600/91 msec; section thickness, 2.6 mm; FOV, 250) was performed with diffusion-module. Diffusion was measured by using b values of 1000 s/mm^2. After a routine MR examination, a 3D, T1-weighted gradient recalled echo sequence was prescribed to acquire DCE-MRI data. This protocol was performed with parameters (TR/TE, 5.32/1.85; slice thickness, 3.5 mm; FOV, 250; flip angle, 15°). After two acquisitions, a bolus of Gd-diethylenetriaminepenta-acetic acid (Gd-DTPA 0.1 mmol/kg; Magnevist, Bayer, Berlin, Germany) was injected at a rate of 3 ml/s through a 20 G antecubital intravenous line. Bolus injection was performed with an MR-compatible power injector (Spectris; Medrad, Pittsburgh, PA) followed by a 15-ml saline flush. The DCE-MRI was continued for 4.0 minutes after the Gd-DTPA injection.

Image analysis

All images were analyzed by consensus by two genitourinary radiologists (with 6 and 9 years of experience in pelvic MR imaging, respectively) who were all clinical information and the reference standard. A consensus was adopted if different opinions were provided by the two radiologists.

For each cervical cancer evaluated, the following were recorded: tumour volume, lymph node size on MR imaging, and ADC value. Tumour volume was calculated as the summation of all of the areas of the tumour on axial T2-weighted images multiplied by the slice interval [8]. Lymph node size was defined as the maximum diameter measured with a caliper tool on axial T1-weighted images. Apparent diffusion coefficient (ADC) maps were also analyzed qualitatively. Mean values of ADC were measured at the corresponding maps.

For DCE-MRI parameter measurements, pharmacokinetic analysis was carried out using noncommercial software, Omnikinetics (GE Healthcare, Shanghai, China) with the two-compartment Extended Tofts model. A fully automated image-based individualized AIF (iAIF) estimation method was used as the AIF estimation method. The parameters including the volume transfer constant between blood plasma and extracellular-extravascular space (EES) (K^{trans}, min^{-1}), rate constant between EES and blood plasma (K_{ep}, min^{-1}), volume of EES space per unit volume of tissue (V_e) and fractional blood plasma volume per unit volume of tissue (v_p) were derived from the entire ROI for each patient. The radiologists manually drew ROIs along contours of the tumour, covering the whole lesion with the exclusion of the necrosis, peripheral fat and blood vessels based on T2-weighted images as a guide. After each ROI placement, color-coded, pixel-wise, parametric perfusion maps of K^{trans}, K_{ep}, V_e and V_p were generated with sample patients as shown in **Figure 1**.

Follow-up

All patients were routinely examined at 3-6 month intervals for the first 2 years following operation. Patients underwent a thorough physical examination, laboratory analysis, computed tomography (CT) scan and MR examination if necessary to detect recurrent disease. Lymph node recurrence was clinically diagnosed when enlarged lymph nodes were detected as compared with preoperative images. Two-year follow-up was completed for all 58 patients after operation.

Statistical analysis

Statistical analysis was performed using the PASW statistical software (version 18.0; SPSS, Inc., Chicago, IL, USA). Values are presented as mean ± SD. Quantitative data (age, tumour volume, lymph node size, ADC value, DCE-MRI parameters) were compared using the Independent-Samples Test. An χ^2 test FIGO stage, histological type, CEA, distant metastasis was used to compare qualitative data between the groups in terms of lymph node metastasis (+/-). A p value < 0.05 was regarded as significant.

Results

Patients and clinicopathological features

A total of 58 patients were included in the present study. Of those, 38 (65.5%) patients were FIGO stage Ib, 15 were (25.9) stage IIa, 4 were

Table 1. Patient and pathological characteristics

	Lymph node metastasis (28)	Non-lymph node metastasis (30)	*P* value
Median age (range)	44.8±9.2	46.7±9.5	0.432
FIGO stage			0.446
Ib	19	19	
IIa	6	9	
IIb	2	2	
IIIb	1	0	
Histological type			0.259
Squamous cell carcinoma	25	29	
Adenocarcinoma	3	1	
CEA > 4.0 ng/mL	6	2	0.098
Distant metastasis	2	0	0.084

Data are the mean ± standard deviation.

Table 2. Results for MR imaging with and without lymph node metastasis

	Lymph node metastasis (28)	Non-lymph node metastasis (30)	*P* value
Tumour volume (cm^3)	13.6±18.1	9.7±9.3	0.306
Lymph node size on MR imaging (cm)	1.1±0.6	0.9±0.4	0.291
ADC ($\times 10^{-3}$ mm^2/s)	0.694±0.020	0.776±0.035	0.044*

Data are the mean ± standard deviation. *Comparisons of ADC value with and without lymph node metastasis: P < 0.05.

Table 3. Results of pharmacokinetic parameters of dynamic contrast-enhanced MR imaging in tumours with and without lymph node metastasis

	Lymph node metastasis (28)	Non-lymph node metastasis (30)	*P* value
K^{trans} (min^{-1})	1.446±0.129	1.047±0.114	0.023*
K_{ep} (min^{-1})	1.750±0.179	1.732±0.133	0.935
V_e (%)	0.730±0.038	0.571±0.045	0.010*
V_p (%)	0.092±0.031	0.080±0.030	0.770

Data are the mean ± standard deviation. *Comparisons of K^{trans} with and without lymph node metastasis: P < 0.05.

(6.9) stage IIb, and 1 was (1.7) stage IIIb. There were 54 (93.1) cases of squamous cell carcinomas and 4 (6.9) adenocarcinomas. 28 patients (median age, 44.8 years; range, 25-64 years) exhibited lymph node metastasis, and 30 patients (median age, 46.7 years; range, 30-65 years) did not exhibit lymph node metastasis. 6 (21.4) cases had CEA > 4.0 ng/mL in patients with lymph node metastasis, and 2 (6.6) cases had CEA > 4.0 ng/mL in patients without lymph node metastasis. During the two-year follow-up period, there were two cases of distant metastases in patients with lymph node metastasis.

The clinical and pathological characteristics of all 58 patients are shown in **Table 1**.

Radiological results

Table 2 summarizes the size and volume of the tumour between with and without lymph node metastasis. Tumour volume and lymph node size on MR imaging showed no significant difference between the two groups (P > 0.05). Additionally, the ADC value showed a significant difference between the two groups (P < 0.05): ADC value was significantly increased in the tumour with lymph node metastasis (P = 0.044).

Table 3 summarizes the results of DCE-MRI tumour parameters. In the tumour, K^{trans} and v_e value showed a significant difference between the two groups (P < 0.05) (**Figure 1**): K^{trans} value was significantly increased in the tumour with lymph node metastasis (P = 0.023), and v_e value was also significantly increased in the tumour with lymph node metastasis (P = 0.010). However, the k_{ep} and v_p value showed no significant difference between the two groups (P > 0.05).

Discussion

Cervical cancer is clinically classified according to the FIGO clinical staging system, which does not include evaluation of lymph node status. In fact, lymph nodes are the most important site of recurrence for patients with cervical cancer. While there are a number of factors to consider in the calculation of overall and disease-specif-

ic survival, a recent multivariate analysis demonstrated that lymph node metastasis represented the only significant independent prognostic indicator for all outcomes, including overall survival, disease-specific survival, and local recurrence.

In DCE-MRI, a dynamic image acquisition is performed after the administration of an intravenous bolus of gadolinium-based contrast agent. DCE-MRI can accurately reflect tumour angiogenesis. Histologically, lymphatic vessels and blood vessels are both thin walled and tubular structures surrounded by endothelial cells and it is often not possible to accurately differentiate them without elastic tissue staining. As a result, the term "lymphovascular" is usually used [9]. So far, DCE-MRI has been used mostly for breast and brain tumour [10], has a high predictive value for the metastasis and prognosis of tumour, both of which are known to affect the response to and outcome of radiotherapy [11]. In addition, several studies also have reported that DCE-MRI is useful to differentiate the metastatic lymph nodes from benign lymph nodes [12, 13]. However, the correlation between the quantitative parameter of tumour and the lymph node metastases was not unexpected. Our results, using 3T MR equipment with high temporal resolution DCE-MRI, demonstrated that the K^{trans} and V_e value were significantly higher in the tumour with lymph node metastasis than in the tumour without lymph node metastasis, while K_{ep} and V_p value showed no significant difference between the two groups. K^{trans} correlate with vascular permeability, we would propose that leisions with higher vascular permeability are more adherent to lymph node metastasis. In addition, with respect to the contrast agent exchange constant V_e, it has been shown that the loss of function of cell-cell adhesion molecules, such as e-cadherin, is a crucial step in tumour progression, both regional and metastatic [14]. This loss of function leads to a larger interstitial space, which is reflected by a higher V_e value. Consequently, DCE-MRI parameters may potentially be used to differentiate patients whether with or without lymph node metastasis. However, this finding certainly needs to be validated in a greater cohort of patients and interpretation has to be done with care.

Diffusion weighted imaging (DWI) is a noninvasive technique based on molecular diffusion that, when combined with conventional T2WI, enables the assessment of morphologic and physiologic changes in a single examination. It also allows for a quantitative evaluation of ADC from images with different b-values [15, 16]. Rita Lucas et al. [17] found that the combination of T2WI and DWI could predict tumor recurrence with a higher sensitivity. Our results showed that a difference between the two groups was found for the ADC value ($P < 0.05$). It is possible that ADC value is especially sensitive to tumour changes being associated with lymphatic channel dissemination. Similar to DCE-MRI, the approach may serve to provide the surgeon more accurate information at the time of operation, thereby improving the precision of the dissection.

We also evaluated tumour volume and lymph node size on MR imaging and concluded that there is no meaningful statistical correlation between the two groups. CEA as an oncofetal antigen is expressed during embryonic development but not in normal adult tissues. Neoplastic transformation, however, may reinduce CEA expression. A strong correlation between tumour burden and initial serum levels has been reported for cervical carcinoma [18, 19]. A preoperative CEA level ≥ 4.0 ng/ml was reported to be associated with the early distant metastasis [20]. In our study, there was no significant correlation between CEA level and lymph node metastasis ($P > 0.05$). The result is not in line with the finding of other authors, perhaps because of a lack of number in patients.

Despite advances in multimodal therapeutic modalities, prognosis of cervical cancer remains poor [21-23]. The presence of lymph node metastasis has been specifically recognized as an important unfavorable prognostic factor for cervical cancer and a major cause of death [24]. During the two-year follow-up period, there were two cases of distant metastases in patient with lymph node metastasis, and a long-term follow-up are needed to assess the potential of DCE-MRI to predict survival.

There are several limitations in our study. First, our study had a small number of patients. Second, the two-year follow-up period was short, and we did not evaluate the correlation between preoperative DCE-MRI parameters and prognosis. Further studies are needed on

this aspect. Finally, although the tumour have heterogeneous contrast uptake, we used the contrast uptake of the whole ROI within the tumour in the analysis. In future studies, for example, histogram analysis may be recommended to quantify the heterogeneity of intratumor contrast uptake to differentiate between them [6, 25].

In conclusion, our preliminary results suggest that K^{trans} and V_e of DCE-MRI are useful for predicting the probability of lymph node metastasis in cervical cancers, and that the ADC value is an effective and necessary supplementation for predicting lymph node metastasis. As such, the application of this technology has the potential to improve identification of lymph node metastasis, which may improve outcomes in overall survival, disease-specific survival, and recurrence.

Acknowledgements

The manuscript has been professionally reviewed and edited by LetPud. All the authors have no conflict of interest. Contract grant sponsor: the National Natural Science Foundation of China; contract grant number: 81471723.

Disclosure of conflict of interest

None.

Address correspondence to: Zhanlong Ma, Department of Radiology, First Affiliated Hospital of Nanjing Medical University, Nanjing, China. Tel: 13675123420; E-mail: mazhanlong@126.com

References

[1] Jemal A, Bray F, Center MM, Ferlay J, Ward E and Forman D. Global cancer statistics. CA Cancer J Clin 2011; 61: 69-90.

[2] Okazawa M, Mabuchi S, Isohashi F, Suzuki O, Ohta Y, Fujita M, Yoshino K, Enomoto T, Kamiura S and Kimura T. The prognostic significance of multiple pelvic node metastases in cervical cancer patients treated with radical hysterectomy plus adjuvant chemoradiotherapy. Int J Gynecol Cancer 2012; 22: 490-497.

[3] Sakuragi N. Up-to-date management of lymph node metastasis and the role of tailored lymphadenectomy in cervical cancer. Int J Clin Oncol 2007; 12: 165-175.

[4] Semple SI, Harry VN, Parkin DE and Gilbert FJ. A combined pharmacokinetic and radiologic assessment of dynamic contrast-enhanced magnetic resonance imaging predicts response to chemoradiation in locally advanced cervical cancer. Int J Radiat Oncol Biol Phys 2009; 75: 611-617.

[5] Li X, Yin Y, Sheng X, Han X, Sun L, Lu C and Wang X. Distribution pattern of lymph node metastases and its implication in individualized radiotherapeutic clinical target volume delineation of regional lymph nodes in patients with stage IA to IIA cervical cancer. Radiat Oncol 2015; 10: 40.

[6] Nijman HW, Khalifa M and Covens A. What is the number of lymph nodes required for an "adequate" pelvic lymphadenectomy? Eur J Gynaecol Oncol 2004; 25: 87-89.

[7] Ovrebo KM, Ellingsen C, Hompland T and Rofstad EK. Dynamic contrast-enhanced magnetic resonance imaging of the metastatic potential of tumors: a preclinical study of cervical carcinoma and melanoma xenografts. Acta Oncol 2013; 52: 604-611.

[8] Kim JH, Kim CK, Park BK, Park SY, Huh SJ and Kim B. Dynamic contrast-enhanced 3-T MR imaging in cervical cancer before and after concurrent chemoradiotherapy. Eur Radiol 2012; 22: 2533-2539.

[9] Yu J, Xu Q, Huang DY, Song JC, Li Y, Xu LL and Shi HB. Prognostic aspects of dynamic contrast-enhanced magnetic resonance imaging in synchronous distant metastatic rectal cancer. Eur Radiol 2017; 27: 1840-1847.

[10] Farjam R, Tsien CI, Lawrence TS and Cao Y. DCE-MRI defined subvolumes of a brain metastatic lesion by principle component analysis and fuzzy-c-means clustering for response assessment of radiation therapy. Med Phys 2014; 41: 11708.

[11] O'Connor JP, Tofts PS, Miles KA, Parkes LM, Thompson G and Jackson A. Dynamic contrast-enhanced imaging techniques: CT and MRI. Br J Radiol 2011; 84: S112-S120.

[12] Schob S, Meyer HJ, Pazaitis N, Schramm D, Bremicker K, Exner M, Höhn AK, Garnov N, Surov A. ADC histogram analysis of cervical cancer aids detecting lymphatic metastases-a preliminary study. Mol Imaging Biol 2017; 19: 953-962.

[13] Yan S, Wang Z, Li L, Guo Y, Ji X, Ni H, Shen W and Xia S. Characterization of cervical lymph nodes using DCE-MRI: differentiation between metastases from SCC of head and neck and benign lymph nodes. Clin Hemorheol Microcirc 2016; 64: 213-222.

[14] Herzig M, Savarese F, Novatchkova M, Semb H and Christofori G. Tumor progression induced by the loss of E-cadherin independent of beta-catenin/Tcf-mediated Wnt signaling. Oncogene 2007; 26: 2290-2298.

[15] Sala E, Rockall A, Rangarajan D and Kubik-Huch RA. The role of dynamic contrast-enhanced and diffusion weighted magnetic resonance imaging in the female pelvis. Eur J Radiol 2010; 76: 367-385.
[16] Levy A, Caramella C, Chargari C, Medjhoul A, Rey A, Zareski E, Boulet B, Bidault F, Dromain C and Balleyguier C. Accuracy of diffusion-weighted echo-planar MR imaging and ADC mapping in the evaluation of residual cervical carcinoma after radiation therapy. Gynecol Oncol 2011; 123: 110-115.
[17] Lucas R, Lopes DJ and Cunha TM. Added value of diffusion-weighted MRI in detection of cervical cancer recurrence: comparison with morphologic and dynamic contrast-enhanced MRI sequences. Diagn Interv Radiol 2015; 21: 368-375.
[18] Braun P and Leyendecker G. Carcinoembryonic antigen in cervical cancer: a five-year follow-up. Cancer Detect Prev 1983; 6: 249-253.
[19] Zhou X, Wang H and Wang X. Preoperative CA125 and fibrinogen in patients with endometrial cancer: a risk model for predicting lymphovascular space invasion. J Gynecol Oncol 2017; 28: e11.
[20] Volgger B, Aspisirengil C, Genser-Krimbacher E, Ciresa-Koenig A, Daxenbichler G, Fuchs D, Windbichler G and Marth C. Prognostic significance of TPA versus SCC-Ag, CEA and neopterin in carcinoma of the uterine cervix. Cancer Lett 2008; 262: 183-189.
[21] Qiu JT, Abdullah NA, Chou HH, Lin CT, Jung SM, Wang CC, Chen MY, Huang KG, Chang TC and Lai CH. Outcomes and prognosis of patients with recurrent cervical cancer after radical hysterectomy. Gynecol Oncol 2012; 127: 472-477.
[22] Tong YQ, Liu B, Zheng HY, He YJ, Gu J, Li F and Li Y. Overexpression of BMI-1 is associated with poor prognosis in cervical cancer. Asia Pac J Clin Oncol 2012; 8: e55-e62.
[23] Peng X, Wu Z, Yu L, Li J, Xu W, Chan HC, Zhang Y and Hu L. Overexpression of cystic fibrosis transmembrane conductance regulator (CFTR) is associated with human cervical cancer malignancy, progression and prognosis. Gynecol Oncol 2012; 125: 470-476.
[24] Kidd EA, Siegel BA, Dehdashti F, Rader JS, Mutch DG, Powell MA and Grigsby PW. Lymph node staging by positron emission tomography in cervical cancer: relationship to prognosis. J Clin Oncol 2010; 28: 2108-2113.
[25] Harry VN. Novel imaging techniques as response biomarkers in cervical cancer. Gynecol Oncol 2010; 116: 253-261.